Interaction of Lung Surfactant Proteins with Anionic Phospholipids

D. Y. Takamoto,* M. M. Lipp,* A. von Nahmen,* Ka Yee C. Lee,[†] A. J. Waring,[‡] and J. A. Zasadzinski*

*Department of Chemical Engineering, University of California, Santa Barbara, California 93106, [†]Department of Chemistry, University of Chicago, Chicago, Illinois 60637, and [‡]Department of Pediatrics, MLK/Drew University Medical Center and University of California, Los Angeles, California 90059 USA

ABSTRACT   Langmuir isotherms, fluorescence microscopy, and atomic force microscopy were used to study lung surfactant specific proteins SP-B and SP-C in monolayers of dipalmitoylphosphatidylglycerol (DPPG) and palmitoyloleoylphosphatidylglycerol (POPG), which are representative of the anionic lipids in native and replacement lung surfactants. Both SP-B and SP-C eliminate squeeze-out of POPG from mixed DPPG/POPG monolayers by inducing a two- to three-dimensional transformation of the fluid-phase fraction of the monolayer. SP-B induces a reversible folding transition at monolayer collapse, allowing all components of surfactant to remain at the interface during respreading. The folds remain attached to the monolayer, are identical in composition and morphology to the unfolded monolayer, and are reincorporated reversibly into the monolayer upon expansion. In the absence of SP-B or SP-C, the unsaturated lipids are irreversibly lost at high surface pressures. These morphological transitions are identical to those in other lipid mixtures and hence appear to be independent of the detailed lipid composition of the monolayer. Instead they depend on the more general phenomena of coexistence between a liquid-expanded and liquid-condensed phase. These three-dimensional monolayer transitions reconcile how lung surfactant can achieve both low surface tensions upon compression and rapid respreading upon expansion and may have important implications toward the optimal design of replacement surfactants. The overlap of function between SP-B and SP-C helps explain why replacement surfactants lacking in one or the other proteins often have beneficial effects.

INTRODUCTION

Lung surfactant (LS) is a lipid-protein mixture that lines the alveolar air-liquid interface of air-breathing vertebrates and acts to lower surface tension. To work properly, LS must be fluid enough to adsorb quickly to the alveolar interface to form a monolayer. The monolayer thus formed must be rigid enough to promote near zero surface tensions during the alveolar compression accompanying exhalation. At the same time, the monolayer needs to remain fluid enough to respread quickly and reversibly upon inhalation. Based on pure component phase behavior, individual LS components can be classified as either good low surface tension stabilizers or good fluidizers (McConnell, 1991; Möhwald, 1990). However, these properties are mutually exclusive; good low surface tension stabilizers adsorb poorly from solution and respread poorly from a collapsed state, whereas good fluidizers cannot achieve low surface tensions.

The squeeze-out theory of LS function was proposed to account for the dichotomy inherent in the necessary properties of LS monolayers (Bangham et al., 1979; Goerke and Clements, 1986; Shapiro and Notter, 1989; Goerke, 1998). The theory states that fluidizing lipids in LS are present only to facilitate the adsorption of surfactant to the interface. On compression, the fluidizing lipids are selectively removed, or squeezed out, leaving behind a monolayer enriched in lipids that promote low surface tension (Watkins, 1968; Bangham et al., 1979; Hildebran et al., 1979; Hawco et al., 1981; Egbert et al., 1989; Pastrana-Rios et al., 1994). The squeeze-out theory assumes an idealized, immiscible interaction between the saturated (low surface tension stabilizers) and unsaturated (fluidizing) lipid components. This theory has dominated the interpretation of LS experiments and has strongly influenced the design of replacement LS mixtures for the treatment of respiratory distress syndrome (RDS) (Poulain and Clements, 1995; Schwartz et al., 1994; Johansson, 1998; Robertson and Halliday, 1998). However, convincing evidence of squeeze-out has not been shown even in model monolayers, and the eventual fate of the squeezed-out lipids or proteins is equally unknown.

Here we present isotherms, fluorescence microscopy (FM), and atomic force microscopy (AFM) of mixed dipalmitoylphosphatidylglycerol (DPPG) and palmitoyloleoylphosphatidylglycerol (POPG) monolayers with the LS-specific proteins SP-B or SP-C that show the proteins alter the monolayer phase behavior and morphology, thereby eliminating the need for squeeze-out. By comparing these results with other studies on monolayers of widely varying composition, including animal extract surfactants (Ding et al., 2001; Lipp et al., 1998; von Nahmen et al., 1997), these protein-induced morphological transitions appear to be independent of the details of the lipid composition; instead, they depend on coexistence between a liquid-expanded and liquid-condensed phase. Our findings contradict the squeeze-out theory and may provide a more rational way of designing replacement surfactants for treatment of respiratory distress syndrome.

MATERIALS AND METHODS

SP-B is a 78-residue, lipid-associating protein found almost exclusively in mammalian lung surfactant (Hawgood et al., 1998). The native SP-B protein has a net positive charge of 8 (10 cationic and 2 anionic residues), a large fraction of strongly hydrophobic residues, and four amphipathic helical segments that align parallel to an air-water interface (Gordon et al., 1996, 2000). The native human 78-amino-acid sequence (SP-B$_{1-78}$) is shown below. In each sequence, the charged residues are indicated with a $+$ or a $-$ sign:

$$1 \qquad\qquad + \quad ++ \qquad\qquad +25$$
$$\text{NH}_2\text{-FPIPLPYCWLCRALIKRIQAMIPKG}$$

$$+ \qquad\qquad + \qquad\qquad\qquad 50$$
$$\text{ALRVAVAQVCRVVPLVAGGICQCLA}$$

$$-+ \qquad - \qquad + \qquad\qquad + \qquad\quad + 78$$
$$\text{ERYSVILLDTLLGRMLPQLVCRLVLRCS-COOH}$$

$$\text{(native SP-B)}$$

To simplify synthesis and to try to isolate the essential features of SP-B, we synthesized a peptide based on the N-terminus of SP-B (SP-B$_{1-25}$) (Bruni et al., 1991) in addition to the full-length SP-B$_{1-78}$. SP-B$_{1-25}$ is able to duplicate the functions of full-length SP-B (Lipp et al., 1996, 1998; Longo et al., 1993) including the amphipathic α-helix (Gordon et al., 1996, 2000). The sequence is:

$$1 \qquad\qquad + \quad ++ \qquad\quad + 25$$
$$\text{NH}_2\text{-FPIPLPYCWLCRALIKRIQAMIPKG-COOH}$$

$$\text{(SP-B}_{1-25}\text{)}$$

Full-length SP-B$_{1-78}$, SP-B$_{1-25}$, and a fluorescein-labeled version of the peptide, F-SP-B$_{1-25}$ were synthesized by the solid-phase method of Merrifield, with the use of a tert-butyloxycarbonyl strategy or by FastMoc strategies (UCLA Peptide Synthesis Facility) (Lipp et al., 1996). The crude peptides were purified by C4-column (Vydac, Hesperia, CA) reversed-phase high-performance liquid chromatography (HPLC) with a mixture of water, acetonitrile, and 0.1% trifluoroacetic acid (TFA). Solvents from HPLC and ion-pairing agents were removed from the purified peptides by vacuum centrifugation, and the expected molecular mass of the peptide were obtained by fast atom bombardment mass spectrometry or electrospray mass spectroscopy (UCLA Center for Molecular and Medical Sciences Mass Spectrometry). Quantitative amino acid composition for the peptide was determined at the UCLA Protein Microsequencing Facility.

SP-C is a 4.2-kDa, dipalmitoylated, 35-residue peptide, 23 residues of which are hydrophobic. SP-C has a transbilayer orientation similar to that of integral membrane proteins and adopts a α-helical conformation between residues 9 and 34 (Johansson, 1998):

$$+ \quad ** \qquad ++$$
$$\text{NH}_2\text{-LRIPCCPVNLKRLLVVVVVVVLVVVVI}$$

$$\text{VGALLMGL-COOH} \quad \text{(SP-C)}$$

The N-terminal segment includes two palmitoylcysteinyls (asterisks) and is flexibly disordered. The length of the α-helix is $\sim$3.7 nm and orients along the acyl chains of lipids in a monolayer or bilayer environment (Gericke et al., 1997; Johansson, 1998). The hydrophobic character of SP-C and palmitoylation makes native SP-C difficult to synthesize. We synthesized an analog of SP-C, SP-C*ff* (based on work by Byk-Gulden Pharmaceutical, Konstance, Germany) (Ikegami et al., 1998; Ikegami and Jobe, 1998) in

which the palmitoylated cysteines are replaced by phenylalanine residues (asterisks):

$$+ \quad ** \qquad ++$$
$$\text{NH}_2\text{-LRIPFFPVNLKRLLVVVVVVVVLVVVVIVG}$$

$$\text{ALLMGL-COOH} \quad \text{(SP-C}ff\text{)}$$

This mutant protein performs nearly identically to the native SP-C in animal models (Davis et al., 1998; Ikegami et al., 1998; Ikegami and Jobe, 1998) and is significantly easier to synthesize. This mutant is analogous to dog SP-C, which has only a single palmitoylated cysteine, with the second replaced by phenylalanine (Batenburg and Haagsman, 1998).

SP-C*ff* peptide was synthesized using an Applied Biosystems (Foster City, CA) 431A peptide synthesizer employing FastMoc chemistry. The peptide was synthesized using a prederivatized Fmoc-leu-PEG-PS resin (PerSeptive Biosystems, Farmington, MA) having a substitution of 0.18 mmol/g. Residues Gly-33 to Gly-29 were single coupled, whereas the remaining sequence was double coupled to the N-terminus. Cleavage and deprotection of the peptide-resin was carried out in 10 ml of TFA, 0.25 ml of ethanedithiol, 0.5 ml of thioanisole, and 0.5 ml of water mixture for 1.5 h.

The crude peptide was purified by reverse-phase HPLC with a Vydac C 4 column (1 cm $\times$ 20 cm; The Separations Group, Hesperia, CA) using a water-acetonitrile:isopropanol (1:1, v:v) linear gradient with 0.1% TFA as an ion-pairing agent. The molecular weight of the full-length SP-C*ff* was confirmed by MALDI-TOF mass spectrometry using a Voyager RP-RBT2 reflection time of flight mass spectrometer (PerSeptive Biosystems). α-Cyano-4-hydroxycinnamic acid was used as a matrix, and bovine insulin was used as an internal calibration standard.

The proteins or peptides were mixed with the appropriate amounts of saturated DPPG and unsaturated POPG (Avanti, 99%) at typical concentrations of 0.5–1 mg/ml in 3:1 chloroform:methanol (Fisher Spectranalyzed, St. Louis, MO). The fluorescent probe 1-palmitoyl, 6 - (*N*-7-nitrobenz-2-oxa-1,3-diazol-4-yl-)-PG (NBD-PG, Molecular Probes, Eugene, OR) was added at lipid mole ratios of 0.5–1%. The fluorescent probe segregates to disordered or fluid phases, which then appear bright in images, and the probe is absent from the solid or liquid condensed phases, which appear black or dark (Knobler and Desai, 1992). Monolayers were spread onto pure water (Milli-Q, Millipore, Bedford, MA) subphases in a temperature-controlled microfluorescence film balance (Lipp et al., 1997). Selected monolayers were transferred to mica substrates for AFM using a monolayer transfer system that allowed continuous monitoring of the transfer process with the fluorescence microscope (Lee et al., 1998).

A modified Nanoscope III FM (Digital Instruments, Santa Barbara, CA) was used for imaging. A low-resolution fluorescence optical microscope was used to position the AFM tip onto specific regions of the sample (Lee et al., 1998). Once the desired regions were located, AFM imaging was done with a 150 μm $\times$ 150 μm (J) scanner in contact mode. Silicon nitride tips with a spring constant of 0.12 N/m were used. Exerting large forces on the sample was a concern during imaging, so samples were checked often for deformation. This was done by imaging for a few minutes on a smaller region ($\sim$20 μm) and then zooming out to check whether damage had been done to the scanned region.

RESULTS

The area available to a monolayer, *A*, can be decreased by imposing an external surface pressure, π, which lowers the normal air-water surface tension, γ_o, to γ: $\pi = \gamma_o - \gamma$. Measurements of π versus *A* at constant temperature (Fig. 1) are known as isotherms. At large areas per molecule, monolayers are gaseous; the hydrophobic portions of the molecule make significant contact with the
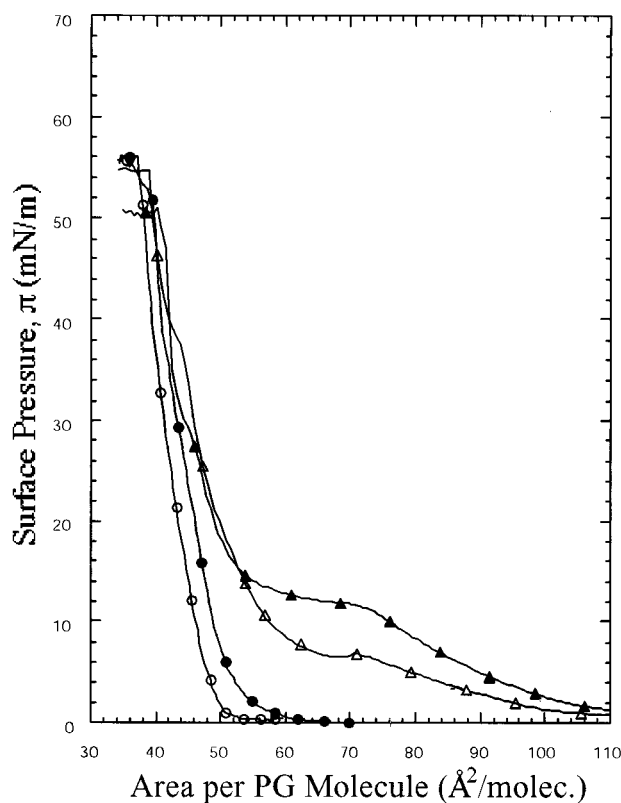
FIGURE 1 Isotherms of dipalmitoylphosphatidylglycerol (DPPG) monolayers on pure water subphases as a function of temperature: ○, 16°C; ●, 23°C; △, 30°C; ▲, 37°C.

water surface but little contact with each other. A gaseous monolayer has little effect on the surface tension, and hence the surface pressure is nearly zero. Above the triple-point temperature for a particular lipid, compression induces the formation of the liquid-expanded (LE) phase from the gaseous phase at low surface pressure. In the LE phase, the hydrophobic parts of the molecules contact each other and lift from the water surface but remain largely disordered and fluid. Further compression leads to a first-order transition to the liquid-condensed (LC) phase, marked by a plateau in the isotherm corresponding to LE and LC coexistence (Fig. 1). The LC phase is characterized by longer-ranged molecular order and lower compressibility than the LE phase. Impurities, such as the fluorescent dye added to visualize the monolayers, preferentially locate in the more disordered LE phase and are expelled from the better ordered LC phase. Below the triple-point temperature, the gaseous phase condenses directly into the LC phase on compression without passing through the intermediate LE phase. A kink in the isotherm at higher compressions marks the second-order phase transition to the better ordered solid (S) phase, in which the area per molecule corresponds to the packing of three dimensional crystals of the amphiphile.

DPPG monolayers

To better illustrate the effects of the proteins on the monolayer phases and morphologies, we first present the phase behavior of DPPG, POPG, and mixed DPPG/POPG films. The triple-point temperature of DPPG on pure water is ~23°C (Fig. 1). Below 23°C, the gaseous phase transforms directly into the LC phase followed by a S phase at higher surface pressure. Above 23°C, DPPG monolayers have a LE phase between the gaseous and LC phases. The plateau in the isotherm indicates LE/LC coexistence; the surface pressure of the plateau increases with temperature. The monolayer collapse pressure, which is the maximum surface pressure or minimum surface tension that the monolayer can support without undergoing a two- to three-dimensional phase transition, decreases from 56 mN/m at 16°C to 51 mN/m at 37°C.

Fluorescence images of DPPG at the triple-point temperature (23°C) show three phases coexisting before the first increase in surface pressure on compression (lift-off): gas, LE, and LC (Fig. 2 A), with the gas phase disappearing upon compression. The fluorescent NBD-PG lipid partitions into the disordered LE and gaseous phases in preference to the better ordered LC phase. However, the fluorescence of NBD-PG is quenched by contact with water. Hence, for gas/LE/LC coexistence, the dark black regions are the gas phase (fluorescence is completely quenched), the medium gray regions are the LC phase, and the bright regions are the
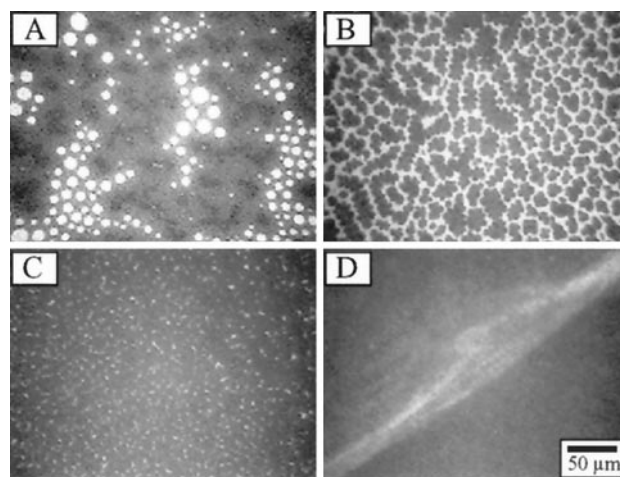
FIGURE 2 FM images taken from a DPPG/1 mol % NBD-PG monolayer on a pure water subphase at 23°C. (A) Three-phase coexistence of gas (dark), liquid-condensed (LC) (gray), and liquid-expanded (LE) (bright) phases. The NBD-PG dye used in quenched when in contact with water, so the gas phase is darkest. The dye is preferentially excluded from the well ordered LC phase in favor of the LE phase. (B) Liquid expanded, liquid condensed phase coexistence at liftoff; the bright phase is LE, the darker phase is LC. The LE phase is usually continuous, with the LC phase forming islands. (C) Solid phase ($\pi = 45$ mN/m); the dye is excluded from the solid phase except at defects which appear bright. (D) Monolayer fracture at the collapse pressure of ~53 mN/m. The monolayer fractures irreversibly, with some material lost to the subphase.

LE phase. A LE/LC coexistence occurs after liftoff (Fig. 2 *B*), with the fraction of fluid phase decreasing upon compression. For LE/LC coexistence, the bright regions are LE phase, and the dark regions are LC phase. For $\pi > 10$ mN/m, the monolayer consisted of a homogeneous solid phase (Fig. 2 *C*). On further compression, the monolayer collapsed by fracturing (Fig. 2 *D*). This process was irreversible; the fractured regions did not respread upon expansion of the monolayer.

Above the triple-point temperature, DPPG monolayers progressed from a gas-LE coexistence at high areas per molecule (Fig. 3 *A*) to a homogeneous LE phase at the liftoff point (Fig. 3 *B*). Upon compression, the LE/LC transition occurred via a first-order nucleation and growth process initiating at a surface pressure that increased with increasing temperature (see Fig. 1). The domains typically contained four to six symmetrically-distributed branching arms (Fig. 3 *C*); this type of growth process is indicative of diffusion-limited growth (Möhwald et al., 1995). Upon further compression, the fluid phase disappeared (Fig. 3 *D*), leaving a

homogeneous LC phase that transformed into a S phase before monolayer collapse (Fig. 3 *E*). Above the triple point, DPPG monolayers collapse by the detachment and solubilization of lipid aggregates into the subphase. Fig. 3 *F* shows the ejected lipid aggregates flowing underneath the monolayer after collapse; these small aggregates came into focus as bright points when the focal plane was scanned into the subphase. This squeeze-out at collapse was irreversible; the solubilized lipid aggregates in the subphase did not reincorporate into the monolayer upon expansion, and the remaining S-phase material at the surface fractured upon expansion to zero surface pressure.

The loss of material at collapse was confirmed by repeated compression of a DPPG monolayer past collapse to an area per molecule of 30 Å^2, expanding to high areas per molecule (or $\pi = 0$ mN/m), then recompressing the same monolayer to collapse (Fig. 4). Each new compression showed an area offset indicating the loss of DPPG from the interface. This behavior continued upon repeated cycling, with the area per molecule at a given surface pressure continuously shifting to lower values. This offset did not occur when DPPG monolayers were cycled to a maximum pressure of 40 mN/m, confirming that the offset was due to material losses during monolayer collapse.

POPG monolayers

Above 20°C, POPG monolayers show temperature-independent phase behavior. The critical point (at which the LC phase does not occur at any surface pressure) for POPG on pure water subphases (pH = 5.5) is ~20°C. Below this temperature, POPG monolayers undergo a high-pressure LE/LC phase transition. For physiologically relevant conditions (above 20°C), POPG monolayers exhibit only the

FIGURE 3 FM images taken from a DPPG/1 mol % NBD-PG monolayer on a pure water subphase at 30°C. (*A*) Gas (dark)-fluid (bright) phase coexistence at high areas per molecule; (*B*) Homogeneous LE phase at the liftoff point where the surface pressure just begins to increase; (*C*) On further compression, the LE/LC transition occurs via a first-order nucleation and growth initiating at a surface pressure ($\pi = 8$ mN/m) that increased with increasing temperature; (*D* and *E*) On further compression, the LE phase disappears leaving a homogenous LC phase that transformed into a homogeneous solid phase (*E*) prior to collapse ($\pi = 40$ mN/m); (*F*) At monolayer collapse, material is ejected from the monolayer into the subphase resulting in bright globular material in the subphase (the image in *F* was taken at a focal plane below the monolayer).

FIGURE 4 Compression-expansion-compression cycling isotherms of a DPPG monolayer on a pure water subphase at 37°C, showing the first (○) and second (●) compression isotherms. The collapsed material is lost irreversibly to the subphase resulting in a systematic offset in area per molecule on subsequent compressions.

LE phase, with the fluid phase existing up to collapse of the monolayer at a surface pressure of ~48 mN/m. As is the case for DPPG above its triple-point pressure, collapse occurs irreversibly by squeeze-out of lipid into the subphase.

Mixed DPPG:POPG monolayers

It has been postulated that squeeze-out occurs in mixed monolayers when one of the components has only a LE phase in its pure form at the same conditions (Fleming and Keough, 1988). At temperatures above 20°C, POPG has only a LE phase; below 20°C, POPG has a LE/LC coexistence at high surface pressure. We therefore examined mixed DPPG:POPG monolayers at temperatures below and above 20°C.

The addition of increasing amounts of POPG had a fluidizing effect on DPPG monolayers at all temperatures. At 16°C is below both the triple-point temperature of DPPG and the critical temperature of POPG. The monolayer compressibility and the fraction of LE phase increased in direct proportion to the amount of POPG added (Fig. 5). Fluores-

cence images showed that adding increasing amounts of POPG lowered the effective triple point of DPPG:POPG mixed monolayers. (The triple point temperature is strictly limited to a pure component monolayer; binary systems can contain three phases over a range of temperatures. We use the term triple point here to refer to mixtures displaying gaseous, fluid, and condensed phases at high areas per molecule.) The 3:1 mol:mol DPPG:POPG monolayers showed a three-phase coexistence at 16°C at zero surface pressure before liftoff (Fig. 6 A), similar to the three-phase coexistence in pure DPPG monolayers at 23°C (see Fig. 2). There was a LE/LC coexistence at liftoff (Fig. 6 B), with the fraction of LC phase increasing with compression (Fig. 6, C and D). The LE phase was transformed completely into LC phase before a surface pressure of 45 mN/m was reached (Fig. 6 E). There was no sign of a plateau in the isotherm at high surface pressures (see Fig. 5), and there was no evidence of squeeze-out via fluorescence microscopy; both DPPG and POPG appeared to remain in the monolayer up to collapse. Collapse occurred via a similar mechanism as in pure DPPG films above the triple point; material was ejected irreversibly into the subphase and was seen to flow underneath the monolayer (bright spots in Fig. 6 F).

Similar behavior was seen as the percentage of POPG was increased; although the fraction of LE phase increased,
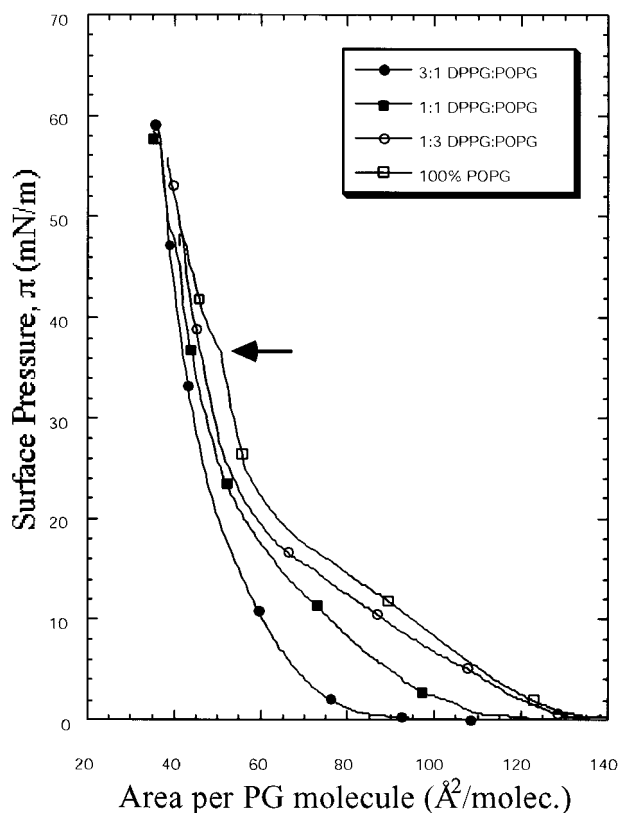
FIGURE 5 Isotherms of mixed DPPG:POPG monolayers on a pure water subphase at 16°C containing (mol:mol): ●, 3:1 DPPG:POPG; ■, 1:1 DPPG:POPG; ○, 1:3 DPPG:POPG; and □, 100% POPG. The arrow indicates the beginning of the fluid- to condensed-phase transition for the 100% POPG monolayer.
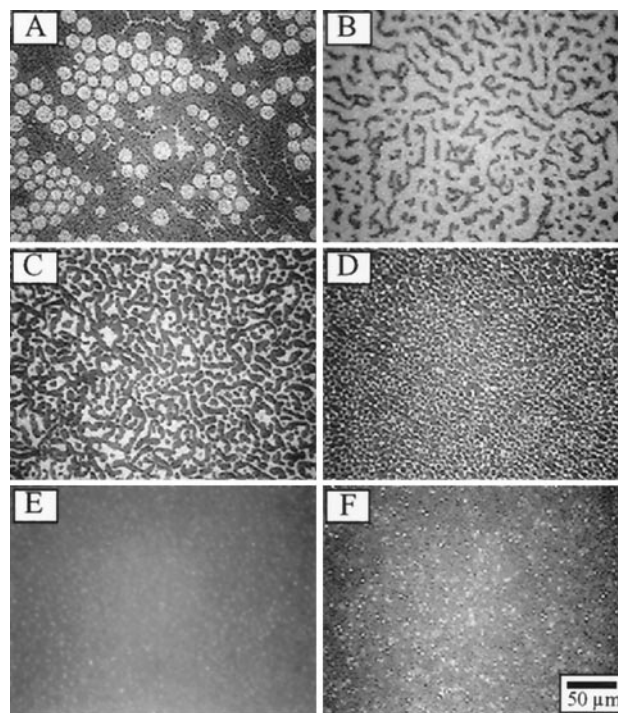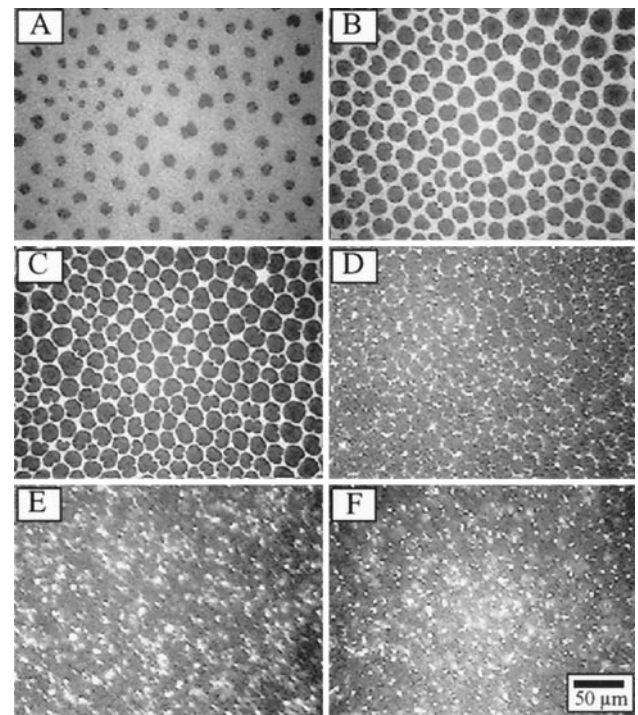
FIGURE 6 FM images from a 3:1 mol:mol DPPG:POPG/1 mol % NBD-PG monolayer on a pure water subphase at a temperature of 16°C, showing the existence of three phases at high areas per molecule (A), fluid and condensed phases remaining at liftoff (B), the conversion of the fluid phase into condensed phase upon compression (C and D), solid phase remaining at high surface pressure ($\pi = 50$ mN/m) (E), and ejected material (bright spots) flowing underneath the monolayer post-collapse (F).

there was still no sign of squeeze-out in the isotherm (no plateau) or the FM images (no removal of material from the monolayer). Even up to 100% POPG, the fluid phase disappeared at a surface pressure below 45 mN/m, leaving a homogeneous sheet of condensed phase (Fig. 6 E). Thus, for all mole ratios at 16°C, the entire LE phase appeared to be converted to LC phase before collapse of the monolayer, with no evidence of material being squeezed out of the monolayer before collapse. Hence, for lipid mixtures in which both lipids have a LC or S phase at high surface pressure before collapse, there is no selective squeeze-out before collapse.

Squeeze-out of fluid phase from mixed DPPG:POPG monolayers before monolayer collapse occurs only above 20°C, the critical temperature for pure POPG. Above 20°C, POPG only has a LE phase up to collapse at ~48 mN/m (Fig. 7). Adding POPG to DPPG results in a plateau in the isotherms for mixed DPPG:POPG monolayers at a surface pressure slightly above the collapse pressure of pure POPG (Fig. 7) (Lipp, 1997). The length of the plateau in the isotherm increased in direct proportion to the fraction of POPG present. On continued compression, the plateau ended, and the surface pressure again increased. The monolayer collapsed at the collapse pressure of pure DPPG under the same conditions. The same basic behavior was observed at temperatures of 30°C and 37°C (Lipp, 1997).

Fluorescence images showed direct evidence of fluid lipid being squeezed out of LE domains at the LE/LC
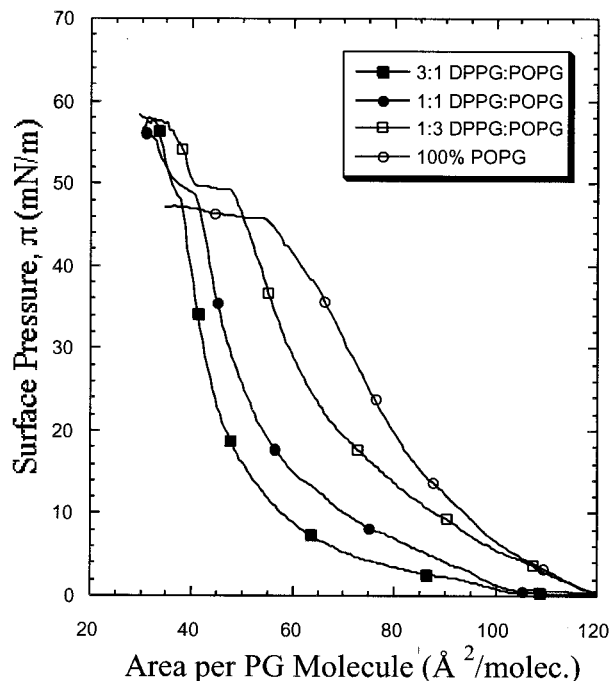
coexistence upon compression (Fig. 8). A 3:1 DPPG:POPG monolayer initially went through a LE to LC coexistence at low surface pressures (Fig. 8 A). The fraction of LC phase increased on compression to higher surface pressures (Fig. 8, B and C). However, a significant amount of LE phase remained, separating LC phase islands up to a surface pressure of 45 mN/m (~18% of the monolayer, as calculated via image analysis, which is significantly less than the 25% expected if all the POPG remained in the LE phase). At the start of the plateau, beginning at a surface pressure of 46 mN/m (see Fig. 7 for the isotherm), the remaining LE phase was squeezed out from the monolayer into the subphase in the form of three-dimensional globular and ribbon-like structures. By the end of the plateau, these structures detached completely from the monolayer and flowed along with the subphase underneath the monolayer (Figs. 8, D–F). This was confirmed by scanning the focus of the microscope into the subphase. These free-floating aggregates did

FIGURE 8 FM images from a 3:1 mol:mol DPPG:POPG/1 mol % NBD-PG monolayer on a pure water subphase at a temperature of 23°C. (A) Nucleation of condensed LC phase from a homogeneous fluid LE phase at a surface pressure of 3 mN/m; (B) Increase in the fraction of (dark) LC phase relative to (bright) LE phase with increasing surface pressure. (C) At the start of the high-pressure plateau (π = 46 mN/m), 18% LE phase remains as calculated via image analysis. This is significantly less than the 25% POPG in the monolayer, suggesting that some fraction of the POPG is in the LC phase. (D and E) Squeeze-out of fluid-phase lipid into the subphase as the monolayer is compressed through the plateau region; (F) Squeezed-out material flowing underneath the monolayer prior to collapse, with the image taken at a focal plane underneath the monolayer. The squeezed-out material does not reincorporate into the monolayer on expansion of the interface.

FIGURE 7 Isotherms of mixed DPPG:POPG monolayers on a pure water subphase at 23°C containing (mol:mol): ●, 3:1 DPPG:POPG; ■, 1:1 DPPG:POPG; ○, 1:3 DPPG:POPG; and □, 100% POPG.

not reincorporate into the monolayer upon expansion; they remained in the subphase even at zero surface pressure. Similar behavior was seen in 1:1 and 1:3 DPPG:POPG monolayers at 23°C; the amount of material squeezed out increased in direct proportion to the amount of POPG initially present in the monolayer (Lipp, 1997).

To test the reversibility of the squeeze-out plateau, cycling isotherms were conducted with 3:1 mol:mol DPPG: POPG monolayers. The monolayer was expanded immediately after the squeeze-out plateau ended, as evidenced by an abrupt increase in the slope of the isotherm (see Fig. 7). The plateau in the isotherm was irreversible; there was an offset on recompression of an area per molecule approximately equal to the extent of the plateau. On the second compression, there was a slight plateau in the isotherm, indicating that some of the POPG retained in the film was squeezed out on the second compression. The isotherms confirm that most of the POPG was lost above the critical temperature of POPG (Lipp, 1997).

The corresponding AFM images of 3:1 DPPG:POPG monolayers transferred to mica substrates (Lee et al., 1998) before and after the high-pressure plateau are shown in Fig. 9. Before the plateau (Fig. 9, *A* and *B*), the lower (darker) LE region surrounds the (brighter) multi-lobed LC domains. The size and shape of the LC domains is consistent with those observed with fluorescence microscopy at the air-water interface, suggesting that little change occurred on transfer to the mica substrate. The height difference between the LC and LE phases is small, ~1.1 ± 0.2 nm, but consistent with the difference in thickness (and compressibility) between the gel and fluid phases for lipids in stacked multilayers (Marsh, 1990). The flower-shaped domains have small holes and defects near the edges, which look like LE phase incorporated near the ends of the solid domains. These features cannot be resolved with optical microscopy and suggest that the solid phase domains trap some of the LE phase. This is consistent with the image analysis of the fluorescence images that showed less than 25% LE phase (Fig. 8).

After the plateau, the POPG-rich fluid phase is squeezed out from the monolayer (Fig. 9, *C* and *D*). The AFM images of monolayers transferred at surface pressures above the plateau show that the condensed-phase domains have been pushed together, and the multi-lobed shapes of the domains are distorted. Due to the deposition technique (Lee et al., 1998), some of the floating material that was expelled from the monolayer was trapped under the deposited monolayer on the substrate; this shows up in the images as globules of material distributed at random across the surface. Only a small amount of LE phase remains; small LC domains are distributed within the LE phase. The remaining LE phase is still lower in height than the LC phase by ~1 nm.

Effects of proteins SP-B and SP-C

FM, AFM, and cycling isotherms show that pure POPG, pure DPPG, and mixed DPPG:POPG monolayers lose material from the interface when compressed to high surface pressure as suggested by the squeeze-out theory. However, once the lipids are squeezed out from the monolayer, they do not return but are lost to the subphase. Moreover, solid-phase monolayers of DPPG collapse irreversibly and cannot respread quickly to cover the interface without fracturing or losing material to the subphase. The properties of the mixed DPPG:POPG monolayers illustrate the difficulty in maintaining the high fluidity necessary for good spreading and the high rigidity necessary for low surface tensions with just lipid mixtures.

Effect of SP-B on squeeze-out

To determine the effect of SP-B and SP-C on phase behavior, similar isotherm, FM, and AFM experiments were conducted on 3:1 DPPG:POPG monolayers containing 10 wt % SP-B$_{1-25}$ or SP-B$_{1-78}$ or 7 wt % SP-Cff. The 3:1 DPPG: POPG ratio is similar to the ratio of saturated to unsaturated lipids in clinical replacement surfactants such as Survanta and Exosurf (Poulain and Clements, 1995; Pison et al., 1996; Goerke, 1998).

The addition of SP-B protein had only a minimal effect on the isotherm of 3:1 DPPG:POPG monolayers at low surface pressure, indicating that the protein did not influence the LE/LC phase transition. However, monolayers incorporating the protein had a significantly higher collapse pressure of ~60 mN/m at both 30°C and 37°C (Fig. 10) (Lipp et al., 1998). A plateau occurred in the isotherm at high surface pressures, although the starting pressure of the plateau was decreased in the presence of protein at a temperature of 37°C (~44 mN/m for SP-B$_{1-25}$ and 38 mN/m for SP-B$_{1-78}$). Fig. 11 *A* shows a fluorescence image of a monolayer of 3:1 DPPG:POPG with 10 wt % fluorescein-labeled SP-B$_{1-25}$. The protein preferentially partitions into the POPG-rich LE phase (Fig. 11 *A*). On compression through the plateau pressure, the LE phase grew progressively brighter and appeared to undergo a two- to three-dimensional transition (Fig. 11 *B*). However, these three-dimensional structures remained centered in the plane of the monolayer, without detaching (Fig. 11 *C*). Thus, instead of being squeezed out, the POPG/SP-B-rich bright fluid phase remained in the interstitial regions in the monolayer up to collapse (Fig. 11 *D*). There was no visible squeeze-out of either lipid or protein from the bright phase.

At collapse, the SP-B protein and peptide led to the creation of large, folded regions that appeared to have the same domain structure and average composition as the bulk of the monolayer (Fig. 11, *E* and *F*). The dark, multi-lobed solid-phase domains remain separated by a continuous, bright LE phase. The monolayer always folded toward the
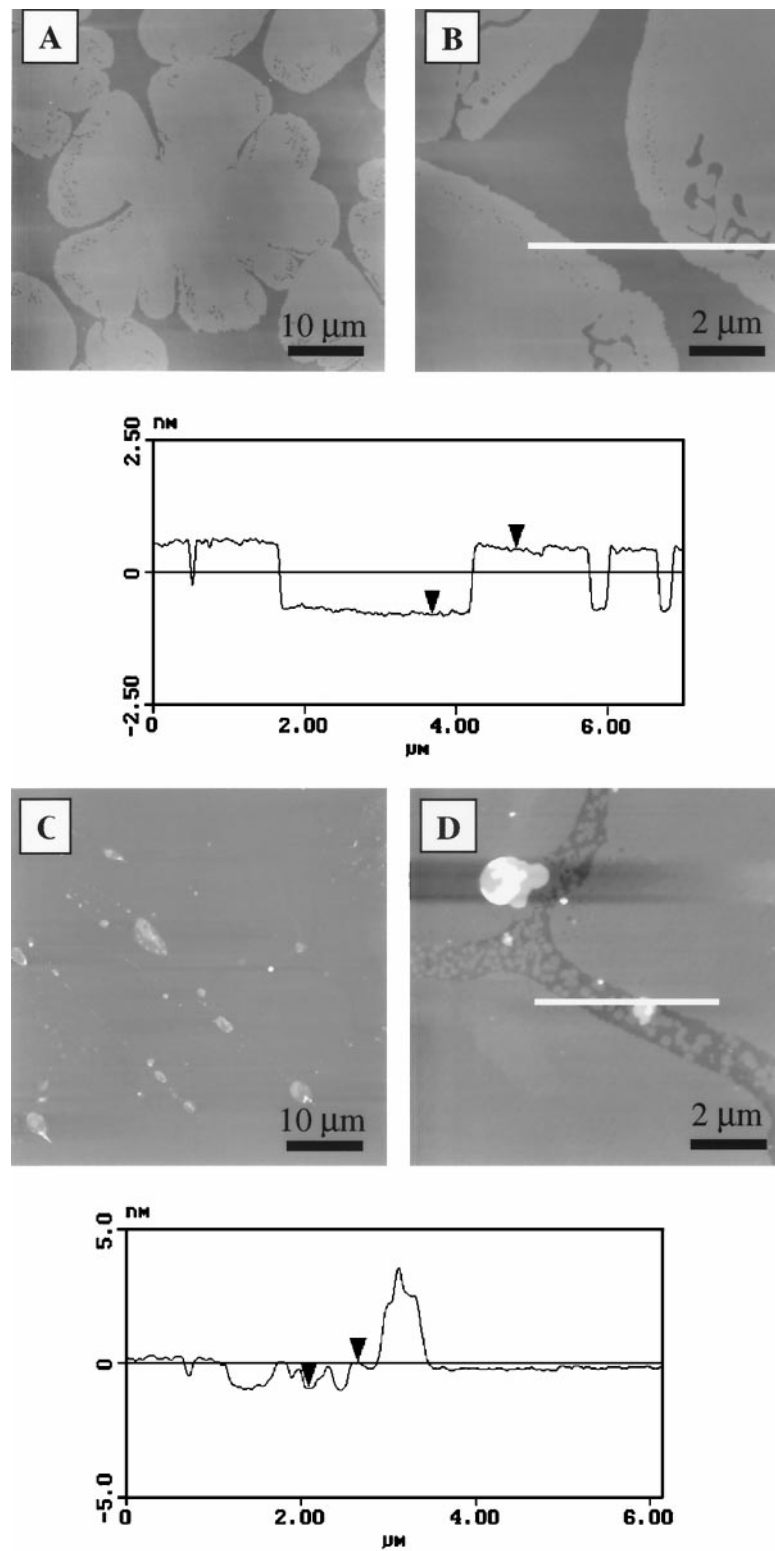
FIGURE 9   AFM images (50 μm and 10 μm on a side) before the high-pressure plateau for the 3:1 DPPG:POPG system. (*A*) Before the plateau ($\pi = $ 40 mN/m), an image of the flower-shaped domain. (*B*) Zoom in on the edge of the domain, to show the defects and holes on the edge of the domains. The white line shows the region of the line trace. The arrows on the height trace show the approximate height difference, which is 1.2 nm. The LC domains are higher than the LE phase, consistent with the expected height and compressibility difference between the solid and fluid chains. (*C*) At surface pressures above the plateau ($\pi = $ 50 mN/m), AFM images show that the material squeezed out from the monolayer is trapped under the monolayer. (*D*) Zoom in on the small remaining fraction of the LE phase. Small islands of LC phase have nucleated even within the remaining LE phase domains. The approximate height difference is 1.0 nm between the LC and LE phases in the monolayer, similar to the difference in heights below the plateau pressure.
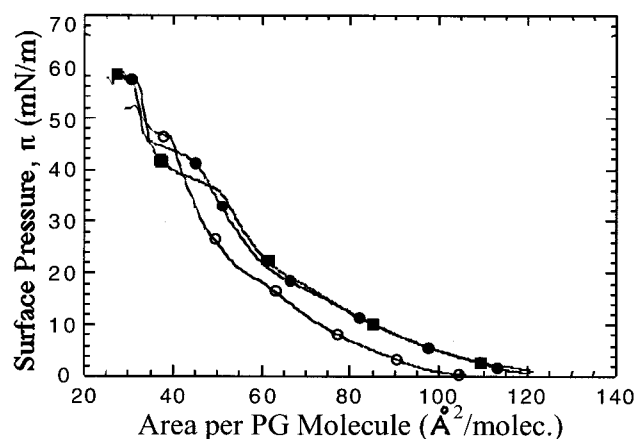
FIGURE 10   Isotherms of 3:1 mol:mol DPPG:POPG monolayers with and without SP-B proteins on a pure water subphase at 37°C, with compositions indicated by: ○, 100% 3:1 DPPG:POPG; ●, 3:1 DPPG:POPG/10 wt % SP-B_{1-25}; and ■, 3:1 DPPG:POPG/10 wt % SP-B_{1-78}.

FIGURE 11   FM images of 3:1 mol:mol DPPG:POPG monolayers containing SP-B_{1-25} protein on pure water subphases at a temperature of 37°C. (A) Image of a monolayer containing 10 wt % F-SP-B_{1-25} at a surface pressure of 30 mN/m, showing the preferential partitioning of the protein into the POPG-rich fluid phase in the interstitial regions; (B–D) Images of monolayers containing 10 wt % SP-B_{1-25}/1 mol % NBD-PG taken through the high-pressure plateau region, showing the retention of the bright fluid phase in the monolayer through the plateau; (E) Image of the same film after collapse, showing the presence of the bright phase network in the monolayer at collapse; (F) Formation of a folded region underneath the subphase (F was taken at a focal plane in the subphase.)

subphase; on expansion, the folded domains quickly reincorporated into the monolayer (Lipp et al., 1998). The folds are a mechanism of maintaining the surfactant near the interface.

Fig. 12, A and B, shows AFM images of a 3:1 DPPG:POPG, 10 wt % SP-B monolayer transferred to a mica substrate (Lee et al., 1998) at a surface pressure below the high-pressure plateau. The solid-phase domains still have the characteristic multi-lobed pattern, and the LE phase is lower in height than the coexisting LC domains, as was the case without SP-B (see Figs. 8–11). One difference is that the LE phase is not uniform but contains many small protrusions that are roughly the same thickness as the LC domains. Fig. 12, C and D, shows AFM images of films transferred to mica at a surface pressure above the plateau. The LC domains are less distorted than without SP-B, and there is a distinct rim of LE phase surrounding and separating the LC islands. The LE domains are now higher than the LC phase, with the heights of the steps on the LE phase corresponding roughly to the bilayer thickness of POPG. Overall, the height difference between the LE and LC domains was 5.0 ± 0.3 nm, and the thicker domains were from 10 to 40 nm high.

Effects of SP-C on squeeze-out

SP-C has a similar effect as does SP-B, as shown in isotherms of a 3:1 DPPG:POPG/7 wt % SP-C*ff* monolayer (Fig. 13 A). As is the case for SP-B, the added SP-C does not alter the normal phase progression of LE/LC coexistence at low surface pressures. Also as for SP-B, there is no evidence that any material is squeezed out from the monolayer, and the second compression is more reversible when the protein is present, even when the film is allowed to

collapse. The collapse pressure increases with added protein, similar to monolayers that included SP-B.

The fluorescence images (Fig. 13 B) show that SP-C has similar general effects as SP-B on lipid monolayers. A bright LE phase separates islands of dark LC phase even up to the collapse pressure. The domains get progressively closer together as the pressure is increased, but no material is lost to the subphase as the high-pressure plateau is reached. However, the shape and size of the solid-phase domains for the SP-C system are very different from the pure lipid and lipid/SP-B system. The LC domains are significantly smaller in the SP-C-containing monolayers (~5 μm) than the LC domains in DPPG/POPG monolayers with and without the SP-B protein (~50–100 μm), and the shape of the domains changes from multi-lobed to round. The SP-C seems to alter the line tension (Knobler and Desai, 1992) between the LE and LC phases and the nucleation rate of the solid phase more than does SP-B, resulting in smaller, more compact domains.

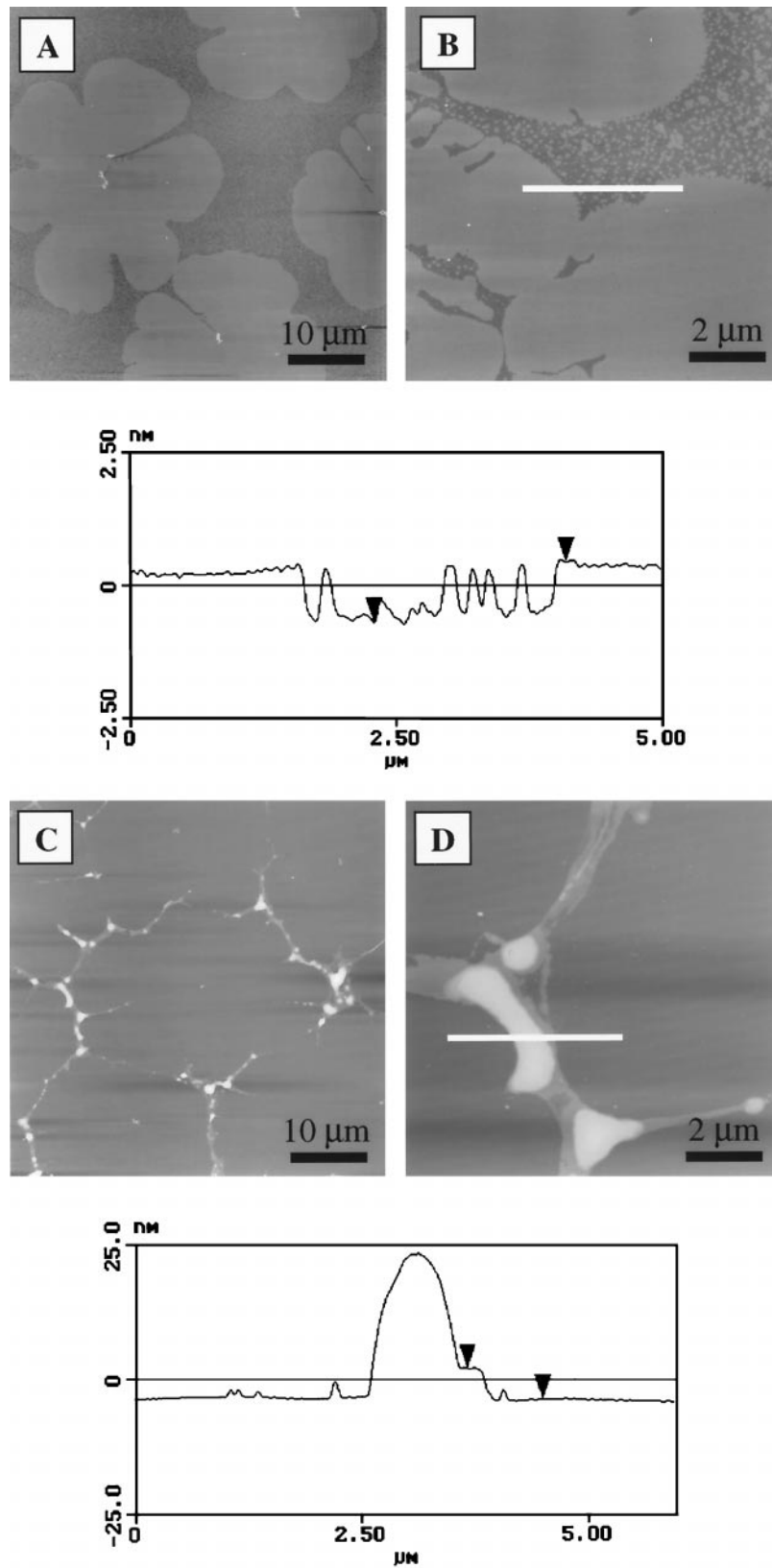Above the plateau in the isotherm ($\pi = 55$ mN/m), AFM images (Fig. 14) of films with SP-C show a distinctly

FIGURE 12 (*A* and *B*) 50 × 50 μm (*A*) and 10 × 10 μm (*B*) contact mode AFM images of 3:1 DPPG:POPG/10 wt % SP-B monolayers transferred to mica substrates at a surface pressure below the high-pressure plateau (π = 40 mN/m). (*A*) Before the plateau, the typical morphology is of flower-shaped LC phase domains in a continuous LE phase; compare with the fluorescence images in Figs. 11, *A–D*. (*B*) Higher magnification of the LE phase, which contains many small solid LC domains. The white line on the image shows the height trace shown below. The arrows on the height trace show the

different morphology than do films with SP-B. A larger fraction of LE phase is retained in the monolayer than with SP-B. A second difference is that the LE phase is uniformly thickened, rather than forming pyramidal layers as shown in Figs. 12, *C* and *D*. The LE domains are ~5–6 nm higher than the surrounding LC domains, again suggesting that these are POPG multilayers. The LE domains are also significantly rougher than the LC domains or the LE domains with SP-B. The LE phase remains continuous and separates the much smaller LC islands. Again, there is no evidence of squeeze-out in these films. Below the plateau pressure, the monolayers have (not shown) a similar morphology as in Fig. 12, *A* and *B*, with the solid domains ~1 nm higher than the LE domains.

Effect of SP-B and SP-C on monolayer collapse

Adding SP-B$_{1-78}$ or SP-B$_{1-25}$ also had a dramatic effect on the collapse mechanism of DPPG:POPG monolayers (Fig. 15) (Lipp et al., 1998). Instead of material being squeezed out from the monolayer, followed by fracture on re-expansion as was the case for both DPPG and DPPG:POPG monolayers, collapse now occurs by a reversible monolayer folding at a higher surface pressure (lower surface tension). At collapse, large regions of the monolayer fold over on itself (Fig. 15 *C*) and form protrusions extending down into the subphase (Fig. 15 *D*). These protrusions consist of multiple folds stacked together that extend several microns into the subphase (the focal planes of the folded regions are below the original monolayer, as shown in Fig. 16). The buckled regions occurred at random across the interface and coexisted with the undeformed, flat monolayer at the collapse pressure of 60 mN/m. Further compression changed the fraction of the monolayer in the folds relative to the flat regions while maintaining a constant surface pressure of 60 mN/m. The continuous network of LE phase surrounding islands of LC or S phase appeared unchanged within the folds; in monolayers with 10 wt % F-SP-B$_{1-25}$ (not shown) the fluid phase appeared bright in the images, indicating that the network remained protein-rich.

On lowering the surface pressure, the collapsed monolayers expanded by reincorporating the folded portions reversibly into the monolayer. The monolayers pulled apart perpendicular to the fold lines, and the folds unzipped back into the monolayer (Fig. 15 *F*). The folds had the same average morphology and composition as the monolayer, and all components rapidly reincorporated into the monolayer upon expansion. Even the normally low-collapse-pressure POPG remained in the monolayer in the presence of SP-B. There was no evidence of any squeeze-out of any of the monolayer components on compression or expansion.

The corresponding AFM images of the folds in the 3:1 DPPG:POPG 10 wt % SP-B monolayers transferred to mica substrates are shown in Fig. 17. As was the case below the collapse pressure (Fig. 12, *C* and *D*), but above the plateau pressure, the LE phase is thicker than the LC phase. Fig. 17 *A* (arrow) shows what may be the initiation of a fold. The solid-phase domains are distorted, and cracks occur within the LE phase. Fig. 17 *B* shows that the smaller folds had heights of ~5–10 nm, which are multiples of the bilayer thickness for DPPG or POPG (Marsh, 1990). The folds did not propagate only through the fluid phase, but often cut through the LC domains. In general, most folds (Fig. 17 *C*) were very high and contained many multilayers (20–100 nm).

SP-C*ff* also induces a folding collapse mechanism as shown in Figs. 13 *B* and 18. The folds were significantly smaller that those induced by SP-B and remained much closer to the interface. Scanning the focal plane of the fluorescence microscope down into the subphase showed that the fold remained near the plane of the interface and did not protrude into the subphase. Increased compression increased the number of folds, but not their size. The folds did extend for several hundred microns across the monolayer, and the folds rapidly reincorporated into the monolayer on expansion. The SP-C folds were usually only one to two bilayers thick as seen in the AFM images in Fig. 18, and although they extended for tens of microns, the folds were usually only ~10 μm wide.

DISCUSSION

The squeeze-out theory is based on three general assumptions: 1) lipids retain their pure component phase behavior in mixtures with other lipids and proteins; 2) saturated and fluid lipids completely phase separate in mixed monolayers to allow for the selective exclusion of the fluid lipid at elevated surface pressures; and 3) after exclusion of the unsaturated lipid, monolayer collapse occurs at the collapse pressure of the saturated component. The squeeze-out theory does not explain the eventual fate of the squeezed-out material, if (and when) the squeezed-out material reincor-

approximate height difference, which is 1.1 nm. The LC domains are higher than the LE phase, and the small domains are the same height as the LC domains. (*C* and *D*) 50 × 50 μm (*C*) and 10 × 10 μm (*D*) contact mode AFM images of 3:1 DPPG:POPG/10 wt % SP-B monolayers transferred to mica substrates at a surface pressure above the high-pressure plateau (π = 55 mN/m). (*C*) The domains of LC phase have lost the flower shape and are more compact; they are still separated by a continuous LE phase, which is now of variable thickness. (*D*) Higher magnification of the LE phase material. The white line on the image shows the region of the line trace. The arrows on the height trace show the approximate height difference, which is 5.2 nm, about the thickness of a bilayer of these lipids. The globule shown is ~30 nm high from the LC domain to its top. The LE phase domains appear to form multilayer patches rather than completely lose the LE phase material to the subphase.
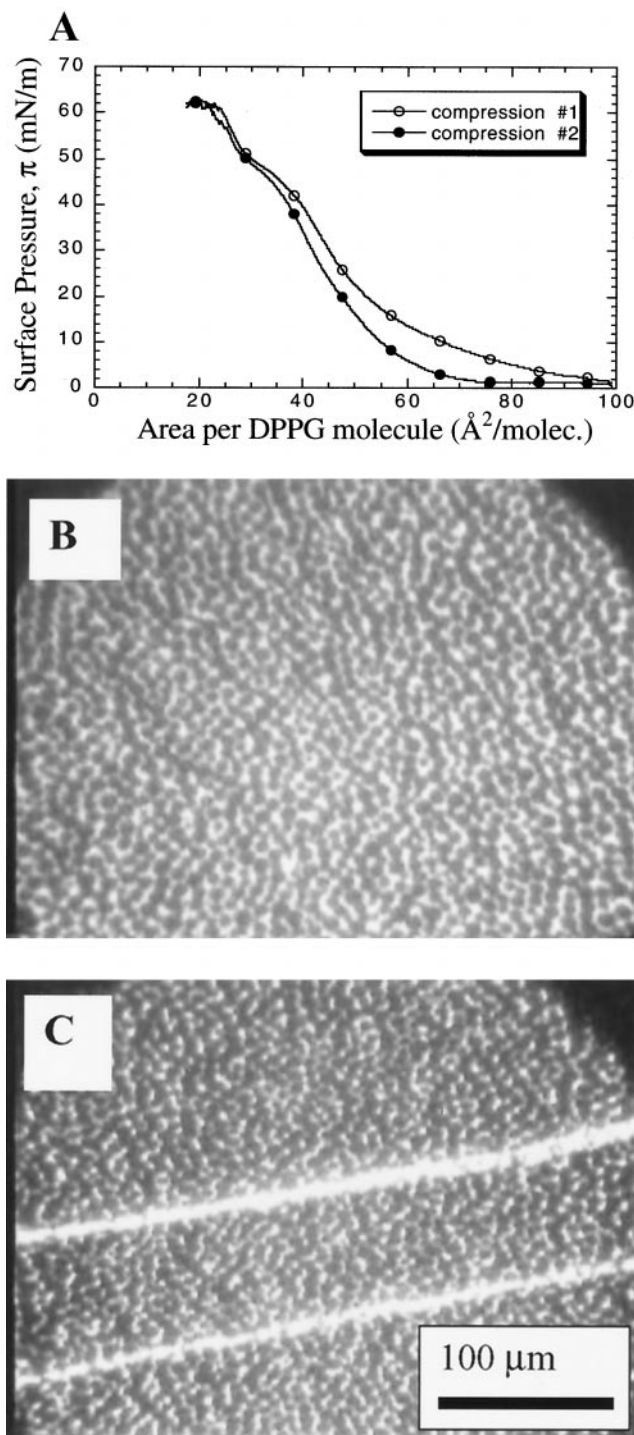
FIGURE 13 (*A*) Cyclic isotherms (compression-expansion-compression) for 3:1 DPPG:POPG/7 wt % SP-C monolayer on pure water at 20°C. Like the isotherm for the SP-B-containing monolayers (Fig. 10), there is less of an offset in molecular area after the first compression. (*B*) Fluorescence micrograph of the monolayer during the high-pressure plateau. SP-C appears to decrease the size of the solid-phase domains significantly compared with monolayer containing SP-B or monolayers with no added protein (compare with Figs. 8 and 11). (*C*) Fluorescence micrograph of the monolayer at collapse. These folds are much smaller than seen with the SP-B system (Fig. 11).

porates into the monolayer, and how the squeeze-out event depends on parameters such as lipid structure, phase behavior, and temperature. More important to LS function, a refined DPPC monolayer cannot mimic the proper activity of LS monolayers in terms of respreadability, reversible hysteresis upon cycling, and incorporation of new material to the interface (Schürch et al., 1995, 1998). LS monolayers need to provide for stable surface tension cycles to allow breathing to occur.

Although the clinical importance of the LS proteins SP-B and SP-C is well established (Tanaka et al., 1986; Poulain and Clements, 1995; Hawgood et al., 1998; Goerke, 1998; Johansson, 1998), the role of these proteins in LS remain ambiguous. It is equally well established that the anionic and unsaturated lipid components of LS are important to the proper function of surfactant at all stages of the compression and expansion cycle (Veldhuizen et al., 1998). Direct imaging with FM and AFM clearly show that the interactions between SP-B, SP-C, and anionic lipids are non-ideal and lead to novel morphologies likely to be important to LS function.

Our results indicate that squeeze-out does occur in mixed saturated/unsaturated lipid systems, but only above the critical temperature of the squeezed-out lipid. The critical temperature of POPG is 20°C; POPG monolayers exist in a fluid LE phase above this temperature at all surface pressures. Regardless of the fraction of POPG added, squeeze-out occurred only in mixed DPPG:POPG monolayers above this temperature. A second key to squeeze-out in lipid mixtures is a LE to LC phase transition at surface pressures near or above the collapse pressure of the pure unsaturated component (Boonman et al., 1987). Whatever LE phase remains at these elevated surface pressures is squeezed out of the monolayer. Although this phase is enriched in POPG in DPPG:POPG mixtures, the phase contains significant amounts of DPPG. Due to their similarity in structure, DPPG and POPG are relatively miscible in mixed monolayers. The isotherms indicate ideal mixing, with the shape of the isotherm changing continuously as the composition ranges from 100% DPPG to 100% POPG. Mixed DPPG: POPG monolayers below the critical point of POPG show a phase progression characteristic of a pure monolayer above its triple point, with LC phase islands nucleating from a homogeneous LE phase at low surface pressure. The LC phase then increases in extent until the monolayer consists entirely of LC phase. Below 20°C, POPG at all mole ratios could pack with DPPG to form a homogeneous condensed phase monolayer at surface pressures in excess of 40 mN/m; there appeared to be no phase separation.

Above the critical point of POPG, the percentage of fluid phase remaining before the plateau in the isotherm increases as a function of temperature. The fraction of LE phase eventually becomes greater than the percentage of POPG present at physiological temperatures, indicating that some DPPG remains in the LE phase. At the plateau in the
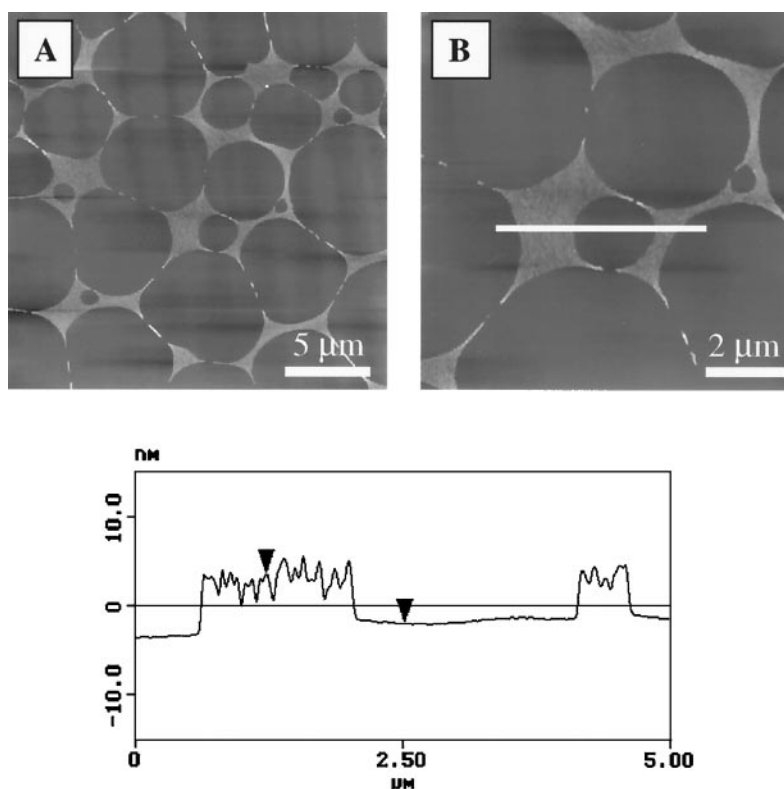
FIGURE 14   (*A* and *B*) 20 × 20 μm (*A*) and 10 × 10 μm (*B*) contact mode AFM images of 3:1 DPPG:POPG/7 wt % SP-C monolayers transferred to mica substrates at a surface pressure above the high pressure plateau (π = 55 mN/m). (*A*) The LC phase is in the form of 1–10-μm round domains compared with the much larger flower-shaped domains in the presence of SP-B. SP-C must alter the line tension between the LC and LE phases, which results in smaller, more rounded domains (Knobler and Desai, 1992; McConnell and De Koker, 1996). The LE phase is much more uniform in height than in the films with only SP-B (see Fig. 12, *C* and *D*) and are, on average, ~6 nm thicker than the LC phase domains. (*B*) 10 μm × 10 μm image. The white line on the image shows the region of the line trace. The arrows on the height trace show the approximate height difference, which is 6 nm. The fluid LE region is higher than the surrounding LC domains. The fluid phase has spikes that increase the roughness, but the entire LE phase has thickened.

isotherm, virtually all of the remaining LE phase transforms into extended bilayer structures that are expelled into the subphase. These structures detach and freely float in the subphase and are not reincorporated into the monolayer on expansion to low surface pressure.

The addition of full-length synthetic SP-B$_{1-78}$, the amino-terminal peptide, SP-B$_{1-25}$, and SP-Cff to mixed DPPG:POPG monolayers eliminates the squeeze-out of the LE phase. Both SP-B and SP-C remain associated with the monolayers at all surface pressures over a wide range of temperatures. Both proteins partition preferentially into the LE phase, resulting in the formation of a protein-rich network that segregates the DPPG-rich LC-phase domains up to the collapse pressure. The solid-phase domains are significantly smaller and more numerous in the SP-C-containing monolayers than the SP-B-containing films, which had domain sizes and shape similar to films with no proteins. This partitioning preference for fluid phases and network formation is also seen in palmitic acid/SP-B monolayers (Lipp et al., 1996) and appears to be a general phenomenon for many amphiphilic proteins (Möhwald, 1990). The presence of the protein network in DPPG:POPG monolayers

increases the collapse pressure of the monolayer to values in excess of 60 mN/m.

Both SP-B and SP-C eliminate the squeeze-out of the POPG-rich LE phase from mixed DPPG:POPG monolayers at physiological temperatures by a similar mechanism. At the plateau that previously corresponded to squeeze-out in the monolayers without protein, both SP-B and SP-C induce a monolayer-to-multilayer transition that appears to anchor the fluid lipids to the interface. In SP-B-containing monolayers, the transition produces areas with multilayer steps and a significant fraction of the LE phase is transformed into multilayers. For SP-C-containing monolayers, the transition produces a uniform thickening of the LE phase, most likely into a uniform trilayer. The fractional coverage of the monolayer with LE phase is greater in SP-C-containing films than SP-B-containing films. Although both proteins are amphiphilic, SP-C contains a hydrophobic α-helical segment that is capable of spanning a lipid bilayer (Johansson, 1998), whereas the helices in SP-B are mainly amphiphilic (Waring et al., 1996). It is likely that there is a change in orientation of the SP-C at high surface pressures, from parallel to normal to the interface that allows the
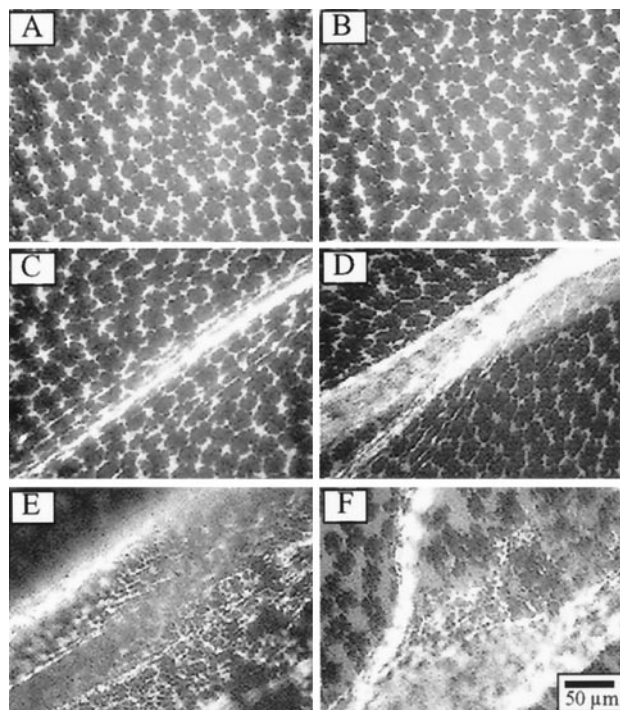
FIGURE 15 Fluorescence microscope images of a 3:1 mol:mol DPPG: POPG monolayer containing 10 wt % SP-B$_{1-78}$ protein on a pure water subphase at a temperature of 30°C. (*A* and *B*) Retention of the bright phase in the interstitial regions in the monolayer through the high-pressure plateau region (*A*) and up to collapse (*B*); (*C*) nucleation; (*D*) growth of a folded region; (*E*) the existence of the same domain morphology within the fold as within the overlying monolayer; (*F*) the unzipping and reincorporation of the folded region upon expansion.

FIGURE 16 FM images of folded protrusions in a 3:1 mol:mol DPPG: POPG/10 wt % SP-B$_{1-78}$/1 mol % NBD-PG monolayer compressed past the collapse point at a temperature of 37°C. The image sequences (*A–C* and *D–F*) display multiple focal planes when the microscope is scanned down from the monolayer (*A* and *D*) into the subphase (*B*, *C* and *E*, *F*) and show that the folds possess the same domain coexistence morphology as the original monolayer.

α-helix to anchor the lipids at the interface (von Nahmen et al., 1997; Gericke et al., 1997). The multilayer transition is reversible for both SP-B- and SP-C-containing films; at low surface pressures the multilayers reincorporate into the monolayer. There is a significantly reduced loss of material as evidenced by more reproducible isotherms with both SP-B and SP-C in the monolayer.

The retention of the fluid-phase network at high surface pressures due to the action of SP-B or SP-C increases the ultimate collapse pressure by altering the mechanism of collapse. The mechanism of monolayer collapse depends primarily on the elasticity and cohesiveness of the monolayer. For single phase, LC or solid monolayers, the semi-crystalline monolayer is apparently too brittle to bend, and collapse occurs by fracture and solubilization of part of the fractured monolayer into the subphase. For the disordered and fluid LE monolayers, collapse occurs by solubilization of material into the subphase, either by molecular solubility or the formation of liquid crystalline aggregates such as vesicles or liposomes. However, monolayers that retain a continuous LE network separating islands of LC or S phase at the collapse pressure, collapse via a reversible buckling in which the monolayer is flexible enough to bend but retains enough cohesion to prevent loss of material to the subphase.
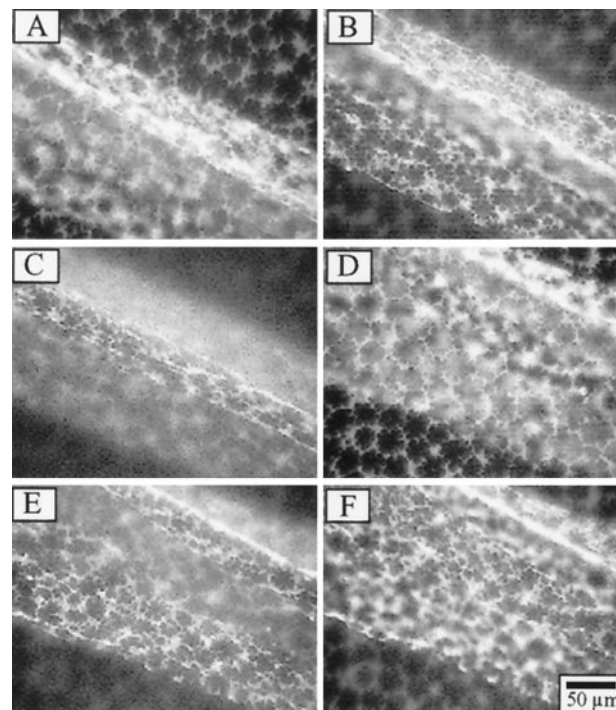
Both SP-B and SP-C induce the folding of the monolayer at collapse. In SP-B-containing films, the folds are many microns wide and extend several microns into the subphase. The domain structure of the monolayer is preserved in the folds, suggesting that the folds have the same composition as the flat monolayer. The folded areas co-exist with the flat monolayer, and the high surface pressure is maintained. On expansion of the monolayer, the folds reversibly reincorporate into the monolayer on expansion. The folds are inherently asymmetric in that folding always occurs into the aqueous subphase. For SP-C-containing films, the folds, like the solid-phase domains, are much smaller and extend only a few bilayers into the subphase. However, these folds are also rapidly reincorporated into the monolayer on expansion, and there is no loss of protein or lipid on continued cycling. The folding process allows collapse to occur at elevated surface pressures while making it possible for the protein and unsaturated lipid components to remain associated with the monolayer, facilitating rapid respreading. This folding and unzipping process explains how LS monolayers can both achieve low surface tensions and respread readily from the collapsed state, without the need to undergo any compositional refinement upon compression. The presence of the protein-containing folds extending into the subphase
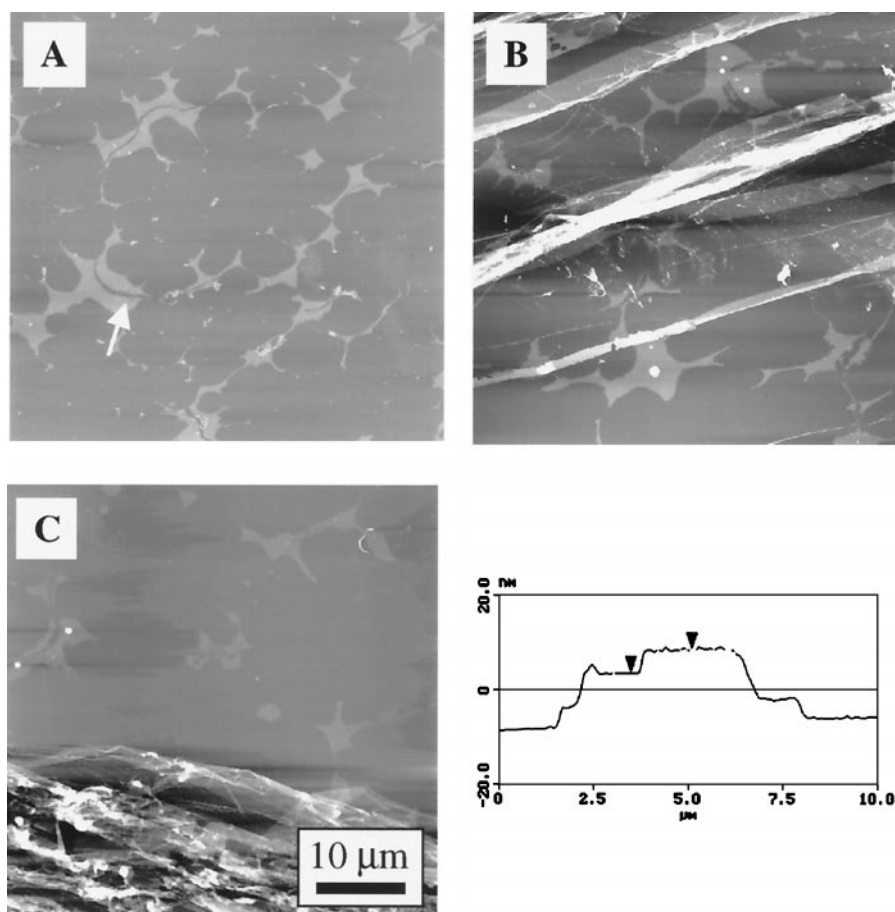
FIGURE 17   Contact mode AFM images (50 μm $\times$ 50 μm) of monolayers transferred to mica substrates after monolayer collapse showing the folded regions for the 3:1 DPPG:POPG/10 % SP-B mixture. (*A*) The LC domains begin to look distorted, and cracks form in the LE phase (*arrow*). These distorted domains and cracks may signify the beginning of the folds. The LE domains are ~6 nm thicker than the LC domains, consistent with multilayer formation. (*B*) Folds can be seen across LC and LE domains. The white line on the image shows the region of the line trace. The arrows on the height trace show the approximate height difference, which is 5 nm (the bilayer thickness). (*C*) Edge of a large folded region. The large folds are on the order of 20–100 nm high.

at high compression may also provide a mechanism for incorporation of new material to the interface upon expansion.

CONCLUSIONS

In this paper, we have shown the first direct images of squeeze-out occurring in mixed saturated/unsaturated phospholipid monolayers, and the elimination of squeeze-out by SP-B or SP-C LS-specific proteins and peptides based on these proteins. Squeeze-out is irreversible in the absence of SP-B or SP-C, with the unsaturated lipid being removed into the subphase and forming stable three-dimensional aggregates that do not reincorporate into the monolayer when the surface pressure is reduced. However, the addition of SP-B or SP-C eliminates squeeze-out by inducing a two-to three-dimensional transition in which the LE phase forms multilayer patches. The fluid network separating the condensed-phase islands remains up to the collapse pressure of

the monolayer. SP-C appears to be somewhat more efficient in stabilizing this transition, likely due to its bilayer-spanning hydrophobic α-helix. The uniform trilayer induced by SP-C is likely more stable than the multi-bilayer patches induced by SP-B and is also more likely to be reincorporated into the monolayer on expansion without loss to the subphase.

This protein-rich network phase remains associated with the monolayer throughout the plateau regions that were traditionally identified as squeeze-out plateaus in LS monolayers. The network phase persists up to collapse of both DPPG and 3:1 DPPG:POPG monolayers, changing the collapse mechanism from the irreversible loss of material to the subphase to a reversible folding event. The folding process allows collapse to occur at elevated pressures while allowing the protein and unsaturated lipid to remain in the monolayer to facilitate the respreading of the monolayer upon subsequent expansion. SP-B leads to a much more dramatic folding event than does SP-C; the SP-B folds are many
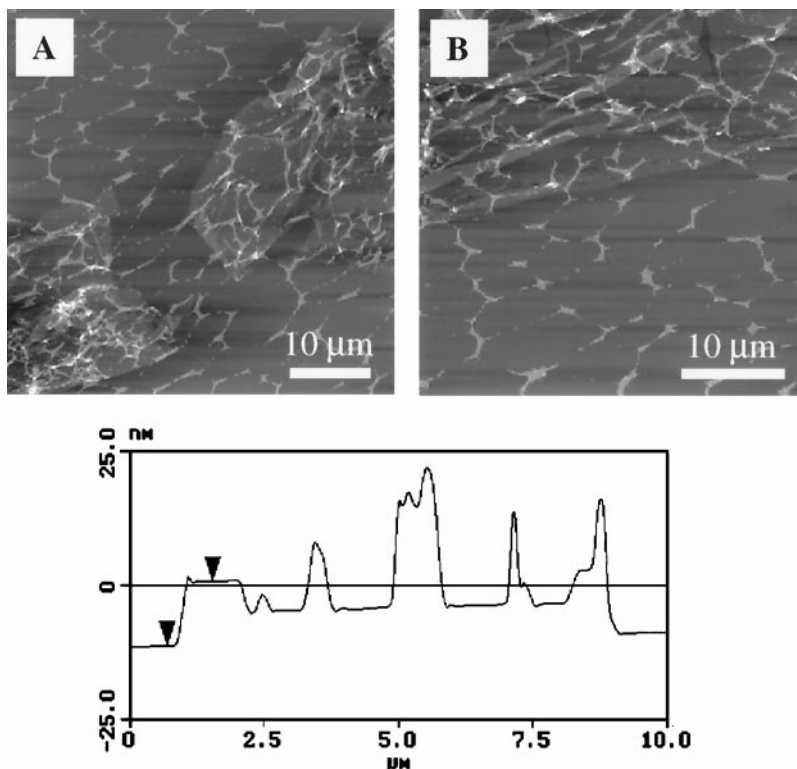
FIGURE 18   Contact mode AFM images of monolayers transferred to mica substrates after monolayer collapse showing the folded regions for the 3:1 DPPG:POPG/7 wt % SP-C system. (*A*) 40 μm $\times$ 40 μm image showing a folded region. This fold has a break in it. The white line shows the regions of the height trace below. Most of the folds consist of no more than one or two bilayers of surfactant. The LE phase (light gray), as in Fig. 14, is $\sim$5 nm thicker than the LC phase domains (dark gray). (*B*) 50 μm $\times$ 50 μm image of a fold. Compared with the folds made by the SP-B protein, the SP-C-generated folds are shorter and narrower. The arrows on the height trace show the approximate height difference, which is 12 nm (twice the bilayer height). The other features are spikes on the folds, probably from the POPG/protein-rich phase as in Fig. 14.

microns in extent and maintain the same domain structure throughout. These SP-B-induced protrusions resulting from the folding process may also act as docking sites for the incorporation of new material to the interface (Oosterlaken-Dijksterhuis et al., 1991).

Although Langmuir monolayers at the air-water interface are taken to be good model systems for studies of lung surfactants and other amphiphilic molecules, care is necessary to extrapolate Langmuir monolayer behavior to lung surfactant behavior in vivo. However, general correlations between in vitro and in vivo behavior are starting to emerge. From this study, one of the key roles of the LS-specific proteins SP-B and SP-C is to retain the unsaturated and anionic lipid components in mixed monolayers up to and even through monolayer collapse. This self-assembly-type process likely occurs in the native LS monolayer. The proteins allow the unsaturated and anionic lipid components to form a continuous network around condensed-phase domains. These morphologies allow low surface tensions while easing the respreadability of the monolayer and facilitating the incorporation of new material to the alveolar interface. The mechanism of collapse is altered from fracture and solubilization to a reversible folding. No squeeze-

out is necessary to obtain low surface tensions. These results may also have important implications for the design of replacement surfactant formulations. Increased percentages of anionic and fluidizing lipids could be added to improve the spreading properties of replacement mixtures, while simple and inexpensive peptide sequences that fully mimic native SP-B or SP-C could be added to allow for low surface tensions to be attained reversibly in the lungs.

REFERENCES

Bangham, A., C. Morley, and M. Phillips. 1979. The physical properties of an effective lung surfactant. *Biochem. Biophys. Acta.* 573:552–556.

Batenburg, J. J., and H. P. Haagsman. 1998. The lipids of pulmonary surfactant: dynamics and interactions with proteins. *Prog. Lipid Res.* 37:235–276.

Boonman, A. A., F. H. Machiels, A. F. Snik, and J. Egberts. 1987. Squeeze-out from mixed monolayers of DPPC and egg phosphatidylglycerol. *J. Colloid Interface Sci.* 120:456–468.

Bruni, R., H. Taeusch, and A. Waring. 1991. SP-B: lipid interactions of synthetic peptides representing the amino-terminal amphipathic domain. *Proc. Natl. Acad. Sci. U.S.A.* 88:7451–7455.

Davis, A. J., A. H. Jobe, D. Hafner, and M. Ikegami. 1998. Lung function in premature lambs and rabbits treated with a recombinant SP-C surfactant. *Am. J. Respir. Crit. Care Med.* 157:553–559.

Ding, J., D. Takamoto, A. von Nahmen, M. M. Lipp, K. Y. C. Lee, A. J. Waring, and J. A. Zasadzinski. 2001. Distinct roles of lipids and proteins in lung surfactant monolayers. *Biophys. J.* 80:2262–2272.

Egbert, J., H. Sloot, and A. Mazure. 1989. Minimal surface tension, squeeze-out and transition temperatures of binary mixtures of dipalmitoylphosphatidylcholine and unsaturated phospholipids. *Biochim. Biophys. Acta.* 1002:109–113.

Fleming, B., and K. M. W. Keough. 1988. Surface respreading after collapse of monolayers containing major lipids of pulmonary surfactant. *Chem. Phys. Lipids.* 49:81–86.

Gericke, A., C. R. Flach, and R. Mendelsohn. 1997. Structure and orientation of lung surfactant SP-C and L-a DPPC in aqueous monolayers. *Biophys. J.* 73:492–499.

Goerke, J. 1998. Pulmonary surfactant: functions and molecular composition. *Biochim. Biophys. Acta.* 1408:79–89.

Goerke, J., and J. A. Clements. 1986. Alveolar surface tension and lung surfactant. *In* Handbook of Physiology, Section 3: The Respiratory System, Vol. III: Mechanics of Breathing (Part I). A. P. Fishman, editor. American Physiological Society, Bethesda, MD. 247–261.

Gordon, L. M., S. Horvath, M. Longo, J. A. Zasadzinski, H. W. Taeusch, K. Faull, C. Leung, and A. J. Waring. 1996. Conformation and molecular topography of the N-terminal segment of surfactant protein B in structure-promoting environments. *Protein Sci.* 5:1662–1675.

Gordon, L. M., K. Y. C. Lee, M. M. Lipp, J. A. Zasadzinski, F. J. Walther, M. A. Sherman, and A. J. Waring. 2000. Lipid conformation of the N-terminal segment of surfactant protein B determined with C13-enhanced Fourier transform infrared spectroscopy. *J. Peptide Res.* 55: 330–347.

Hawco, M. S., P. J. Davis, and K. M. W. Keough. 1981. Lipid fluidity in lung surfactant: monolayers of saturated and unsaturated lecithins. *J. Appl. Physiol.* 51:509–515.

Hawgood, S., M. Derrick, and F. Poulain. 1998. Structure and properties of surfactant protein B. *Biochim. Biophys. Acta.* 1408:150–160.

Hildebran, J. N., J. Goerke, and J. A. Clements. 1979. Pulmonary surface film stability and composition. *J. Appl. Physiol.* 47:604–611.

Ikegami, M., A. D. Horowitz, J. A. Whitsett, and A. H. Jobe. 1998. Clearance of SP-C and recombinant SP0C in vivo and in vitro. *Am. J. Physiol.* 274:L933–L939.

Ikegami, M., and A. H. Jobe. 1998. Surfactant protein-C in ventilated premature lamb lung. *Pediatr. Res.* 44:860–864.

Johansson, J. 1998. Structure and properties of surfactant protein C. *Biochim. Biophys. Acta.* 1408:161–172.

Knobler, C. M., and R. C. Desai. 1992. Phase transitions in monolayers. *Annu. Rev. Phys. Chem.* 43:207–236.

Lee, K. Y. C., M. M. Lipp, D. Y. Takamoto, E. Ter-Ovanesyan, and J. A. Zasadzinski. 1998. From free-standing to transferred films: an apparatus for the continuous monitoring of surface morphology via fluorescence and atomic force microscopy. *Langmuir.* 14:2567–2572.

Lipp, M. M. 1997. A microscopy study of model lung surfactant monolayers. Ph.D. Thesis. University of California, Santa Barbara, CA. 282 pages.

Lipp, M. M., K. Y. C. Lee, D. Y. Takamoto, J. A. Zasadzinski, and A. J. Waring. 1998. Coexistence of buckled and flat monolayers. *Phys. Rev. Lett.* 81:1650–1653.

Lipp, M. M., K. Y. C. Lee, A. J. Waring, and J. A. Zasadzinski. 1997. Design and performance of an integrated fluorescence, polarize fluorescence, and Brewster angle microscope/Langmuir trough system for the study of lung surfactant monolayers. *Rev. Sci. Instrum.* 68:2574–2582.

Lipp, M. M., K. Y. C. Lee, J. A. Zasadzinski, and A. J. Waring. 1996. Phase and morphology changes induced by SP-B protein and its amino-terminal peptide in lipid monolayers. *Science.* 273:1196–1199.

Longo, M., A. Bisagno, J. Zasadzinski, R. Bruni, and A. Waring. 1993. A function of lung surfactant protein SP-B. *Science.* 261:453–456.

Marsh, D. 1990. CRC Handbook of Lipid Bilayers. CRC Press, Boca Raton, FL.

McConnell, H. 1991. Structures and transitions in lipid monolayers at the air-water interface. *Annu. Rev. Phys. Chem.* 42:171–195.

McConnell, H. M., and R. De Koker. 1996. Equilibrium thermodynamics of lipid monolayer domains. *Langmuir.* 12:4897–4904.

Möhwald, H. 1990. Phospholipid and phospholipid-protein monolayers at the air/water interface. *Annu.Rev. Phys. Chem.* 41:441–476.

Möhwald, H., A. Dietrich, C. Böhm, G. Brezesinski, and M. Thoma. 1995. Domain formation in monolayers. *Mol. Membr. Biol.* 12:29–38.

Oosterlaken-Dijksterhuis, M., H. Haagsman, L. van Golde, and R. Demel. 1991. Interaction of lipid vesicles with monomolecular layers containing lung surfactant proteins SP-B and SP-C. *Biochemistry.* 30:8276–8281.

Pastrana-Rios, B., C. R. Flach, J. W. Brauner, A. J. Mautone, and R. Mendelsohn. 1994. A direct test of the "squeeze-out" hypothesis of lung surfactant function. External reflection FTIR at the air-water interface. *Biochemistry.* 33:5121–5127.

Pison, U., R. Herold, and S. Schürch. 1996. The pulmonary surfactant system: biological functions, components, physicochemical properties and alterations during lung disease. *Colloids Surfaces.* 114:165–184.

Poulain, F. R., and J. A. Clements. 1995. Pulmonary surfactant therapy. *West. J. Med.* 162:43–50.

Robertson, B., and H. L. Halliday. 1998. Principles of surfactant replacement. *Biochim. Biophys. Acta.* 1408:346–361.

Schürch, S., F. H. Y. Green, and H. Bachofen. 1998. Formation and structure of surface films: captive bubble surfactometry. *Biochim. Biophys. Acta.* 1408:180–202.

Schürch, S., R. Qanbar, H. Bachofen, and F. Possmayer. 1995. The surface-associated surfactant reservoir in the alveolar lining. *Biol. Neonate.* 67:61–76.

Schwartz, R., M. Anastasia, M. Luby, J. Scanlon, and R. Kellogg. 1994. Effect of surfactant on morbidity, mortality, and resource use in newborn infants weighing 500 to 1500 g. *N. Engl. J. Med.* 330:1476–1480.

Shapiro, D. L., and R. H. Notter. 1989. Surfactant Replacement Therapy. Liss, New York.

Tanaka, Y., T. Tsunetomo, A. Toshimitsu, K. Masuda, K. Akira, and T. Fujiwara. 1986. Development of synthetic lung surfactants. *J. Lipid Res.* 27:475–485.

Veldhuizen, R., K. Nag, S. Orgeig, and F. Possmayer. 1998. The role of lipids in pulmonary surfactant. *Biochim. Biophys. Acta.* 1408:90–108.

von Nahmen, A., M. Schenk, M. Sieber, and M. Amrein. 1997. The structure of a model pulmonary surfactant as revealed by scanning force microscopy. *Biophys. J.* 72:463–469.

Waring, A. J., K. Faull, C. Leung, M. Chang-Chien, P. Mercado, W. Taeusch, and L. Gordon. 1996. Synthesis, secondary structure and folding of the bend region of lung surfactant protein B. *Peptide Res.* 9:28–31.

Watkins, J. C. 1968. The surface properties of pure phospholipids in relation to those of lung extracts. *Biochim. Biophys. Acta.* 152:293–306.